Preprints.org

Article

Not peer-reviewed version

Laser Metal Deposition of WC-NiCrBSi Powders on Gas Carburization Steels Used in Mining Industry

M Kalyan Phani * and Varun Kumar Kurapati

Posted Date: 7 November 2023

doi: 10.20944/preprints202311.0486.v1

Keywords: Surface engineering; Mining tools; harsh environments; microstructure; laser metal deposition; gas carburizing; metallurgical bond; heat-affected zone; metallurgical defects; durability; performance optimization

Article

Laser Metal Deposition of WC-NiCrBSi Powders on Gas Carburization Steels Used in Mining Industry

K. Varun Kumar, M. Kalyan Phani *

Department of Metallurgical Engineering, OP Jindal University, Raigarh- 496109, Chhattisgarh, India
* Correspondence: kalyan.makkuva@opju.ac.in

Abstract: The fusion of surface-modified steel with tungsten carbide (WC) and NiCrBSi powder through laser metal deposition has emerged as a formidable strategy for fortifying components against wear and corrosion in extreme operating environments. Meticulous selection of WC content, innovative pre-alloying techniques, and precise control of laser metal deposition profoundly influence the mechanical properties and microstructural evolution of WC-NiCrBSi coatings applied to surface-enriched commercial alloy steel (805M2, 832M13, and 827M40). These tailored coatings exhibit exceptional resilience, ideal for harsh industrial settings in Oil and gas drilling, petrochemical, and Mining sectors. Advanced materials testing techniques, including scanning electron microscopy, light optical microscopies, and microhardness testing, unveil the innate hardness attributes, with findings highlighting the unassailable fortitude of the Mixed matrix layer's side face. The amalgamation of these testing methodologies with laser metal deposition promises an unparalleled path to extend the operational lifespan of critical components in challenging working conditions. The research horizon for WC-NiCrBSi coatings remains broad, with the potential to enhance durability, operational efficiency, and cost-effectiveness across diverse applications.

Keywords: Surface engineering; Mining tools; harsh environments; microstructure; laser metal deposition; gas carburizing; metallurgical bond; heat-affected zone; metallurgical defects; durability; performance optimization

---

1. Introduction

In the realm of demanding mechanical environments, where components are subjected to severe abrasion, exalted wear, and corrosive atmospheres, the operation of mechanical components necessitates a superlative blend of mechanical attributes and precision in dimensional fidelity [1]. Unfortunately, these components, when exposed to such austere and arduous conditions, exhibit a propensity for expedited degradation. The etiology of mechanical failure in such scenarios, accounting for 70–80% of cases, can be attributed to the deleterious effects of fatigue stress, surface abrasion, corrosion, and wear [2]. This imperatively highlights the need for superlative surface and interface mechanical properties, inclusive of applied coatings, to extend the operational lifespan of these components.

To address these challenges, a considerable research endeavor has led to the development of various surface modification techniques designed to enhance the mechanical properties of metallic components. One such cutting-edge technique, known as laser metal deposition, has emerged as a promising method to impart superior surface attributes to these components [3]. By judiciously applying abrasive metallic powder mixtures, this manufacturing technique has resulted in remarkable improvements in product performance, surpassing non-coated counterparts in field applications [3,4]. These advancements in surface modifications have given rise to composite materials, such as NiCrBSi, which offer exceptional corrosion resistance, fatigue strength, galling resistance, and fretting fatigue resistance [4]. The inclusion of silicon as a fluxing agent has played a crucial role in enhancing the wettability of substrates, ensuring the robust attachment and binding of reinforcing particles [5]. The self-fluxing nature and low melting point of NiCrBSi alloys make them highly desirable as primary binders, enabling effective wetting, attachment, and binding of reinforcing particles [5].

The efficacy of coatings such as NiCrBSi/WC, especially when electrically deposited, has been studied in detail, revealing significant improvements in wear resistance upon the incorporation of WC. Further insights into the microstructures of these coatings before and after WC decomposition have shed light on the formation of herringbone and lamellar shaped carbides [2,5]. This paper delves into a comprehensive investigation of laser-deposited microstructures and mechanical attributes of NiCrBSi and WC coatings. The research explores the role of laser metal deposition (LMD) in the mining sector, where the fortification and toughening of the underlying Ni-matrix binder within the self-fluxing alloy emerge as complementary outcomes of incorporating WC pre-alloyed with NiCrBSi. The concurrent melting of both binders by the laser heat source yields a multi-matrix alloy surpassing the innate characteristics of the original binders, unveiling the advantageous role that hard WC plays in mitigating abrasion rates. Furthermore, the dilution of WC by the direct laser beam has been appreciably curtailed through amalgamation with a Ni-self-fluxing alloy. This research represents a significant step forward in enhancing the durability of mechanical components in challenging and demanding environments, with potential applications in the mining industry and beyond.

2. Materials and Methods

This Materials and Methods section outlines the materials used, the surface modification techniques, coating compositions, the laser cladding process, microstructure analysis, mechanical testing, and the experimental design employed in the study. It provides a clear overview of the research methodology used to investigate the impact of LMD on steel materials in demanding mechanical environments. This Materials and Methods section outlines the materials used, the surface modification techniques, coating compositions, the laser cladding process, microstructure analysis, mechanical testing, and the experimental design employed in the study. It provides a clear overview of the research methodology used to investigate the impact of LMD on steel materials in demanding mechanical environments.

Coating Materials

The primary focus of this study revolves around the development and characterization of NiCrBSi and WC coatings. The following materials were utilized:

- NiCrBSi Alloy: A self-fluxing alloy known for its low melting point and advantageous properties, including corrosion resistance, fatigue strength, galling resistance, and fretting fatigue resistance [6–9].
- Tungsten Carbide (WC): An abrasive material employed to enhance wear resistance, abrasive resistance [6–11].
- Notably, a significant discrepancy in melting temperatures was observed between WC (2850°C) and NiCrBSi (1180°C) [11,12,46]. Additionally, WC-Fe displayed almost double the thermal conductivity of nickel, introducing a compelling contrast in thermal behavior.

Substrate Materials

In this study, distinct alloy steels namely 805M2(sample 1), 832M13(sample 2), and 827M40(sample 3), with enriched surface carbon content 0.6% were employed as substrate materials to assess the impact of surface modification on abrasion resistance.

Coating Compositions

To create the NiCrBSi/WC coatings, Pre-Alloyed NiCrBSi-WC Coating, 60% WC and 40% Ni alloy mixer was considered [6–9,16,19,20].

 doi:10.20944/preprints202311.0486.v1

Surface Modification Techniques

The research aims to investigate the effects of laser metal deposition (LMD) on the aforementioned materials. Laser metal deposition is employed to enhance surface attributes, resulting in improved mechanical performance, and it involves the judicious application of abrasive metallic powder mixtures. The LMD process facilitates efficient mixing and alloying of powder chemical elements within the molten pool, driven by Marangoni convection and buoyancy forces [21,22].

Laser Metal Deposition

The laser cladding process was employed to deposit the above-mentioned coatings on the alloy steel substrates as shown in the schematic Figure 1. The intense heating associated with WC in the LMD process led to WC decomposition, precipitating carbon in the form of graphite, followed by the emergence of free carbon and tungsten [23]. This process was carried out at significantly higher melt pool temperatures ranging from 1800 to 2300 °C, leading to pronounced transformations in the coatings.

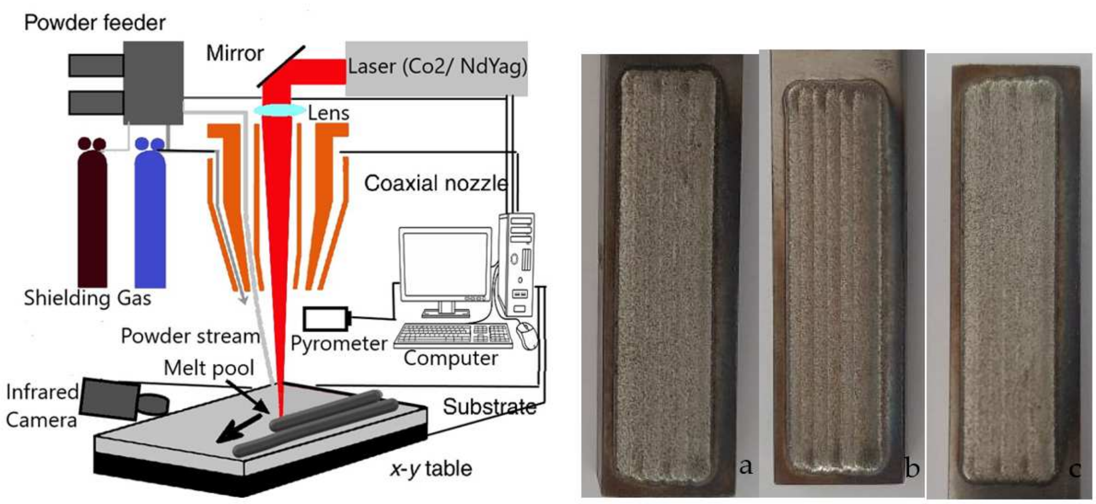

Figure 1. Schematic of Laser Metal Deposition [1]; Figure 1: (**a**) 805M2(sample 1), (**b**)832M13(sample 2), and (**c**) 827M40(sample 3).

Microstructure Analysis

The microstructures of the coatings before and after WC decomposition were examined to gain insights into the structural changes induced by the laser cladding process. Techniques such as optical microscopy, scanning electron microscopy (SEM), and EDS were employed to characterize the microstructural features [24,25].

Mechanical Testing

A LECO hardness tester with a 500 kgf/mm2 stress was used to assess the mechanical properties of the coated materials. Standard operating methods for mechanical testing, such as interface hardness profile and coating depth.

Experimental Design

The experimental design included the deposition of different coating compositions on carbon enriched alloy steel substrates, Pre-alloy mixer of NiCrBSi and WC, and exploring the effects on interface coating and steel. The coatings were characterized and tested to evaluate their performance and mechanical properties.

 doi:10.20944/preprints202311.0486.v1

3. Results and Discussion:

1. Surface Topography and Composition

The deposition process was executed with consistent laser metal deposition parameters, meticulously maintaining power, scanning speed, powder feed rate, overlay composition, and displacement direction as outlined in Table 1.

Table 1. Chemical compositions of feedstock materials.

	Elements (wt.%)			
	Ni	**Cr**	**B**	**Si**
NiCrBSi	78	10-15	1.5-3.0	3-5
WC	60			

Surface Roughness

On the surface, NiCrBSi coatings exhibited a remarkably uniform appearance. As depicted in Figure 1, three prominent peaks, representing adherent powder particles, adorned the surface, resulting in heightened surface roughness (Sa value of 12–15 µm). These resilient particles, primarily composed of partially melted and un-melted constituents, provided a foundation for attached particles [46].

Moreover, an interesting revelation was the transformation in the average surface roughness (Ra), which increased to 1.5–2.5 µm, diverging from the base metal's more modest Ra value of 1–2 µm. This transformation yielded tangible benefits in tribology.

In the laser metal deposition process Table 2, the laser power (P) influences the heat input and material melting, while the scanning speed (S) controls the rate of material deposition. Adjusting the powder feed rate (F), laser diameter (d), overlap, and energy density (E) allows precise control over the resulting material properties and geometry.

2.2. Microstructures post laser metal deposition

The microstructure examination, as presented in Figures 2–4, reveals the outstanding quality of the interface between the substrate and overlay. The absence of cracks or delamination defects underscores the success of the deposition process in achieving a strong bond between the two materials [26,27,29].

The meticulous distribution of WC particles within the Ni matrix is a testament to the precision and effectiveness of the surface modification technique, further contributing to the enhancement of material properties. The presence of minuscule pores, particularly in the interface region, is a point of consideration. While their impact on the overall performance should be assessed, their presence does not diminish the overall achievement in creating a robust and cohesive interface.

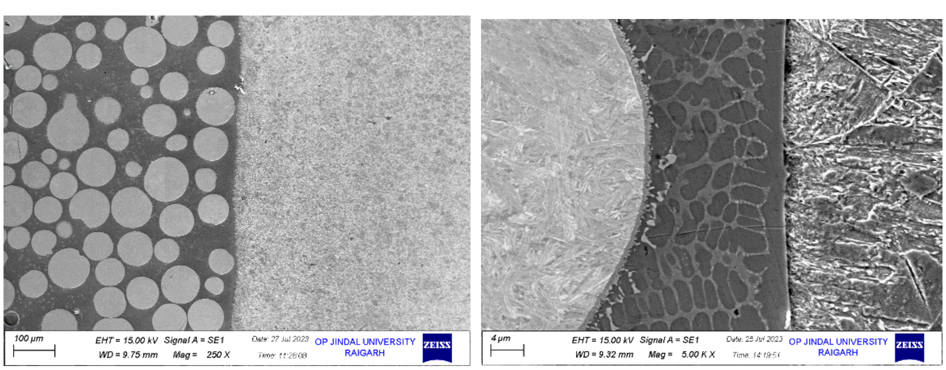

Figure 3. Sample 1: The interface exhibits the metallurgical bonding between steel and Laser Metal Deposition (LMD) of WC-NiCrBSi.

 doi:10.20944/preprints202311.0486.v1

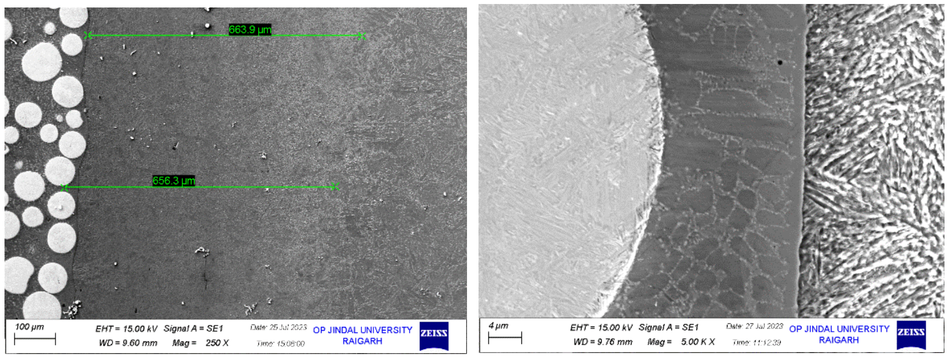

Figure 4. Sample 2: The interface exhibits the metallurgical bonding between steel and Laser Metal Deposition (LMD) of WC-NiCrBSi, indicates gas carburizing case depth.

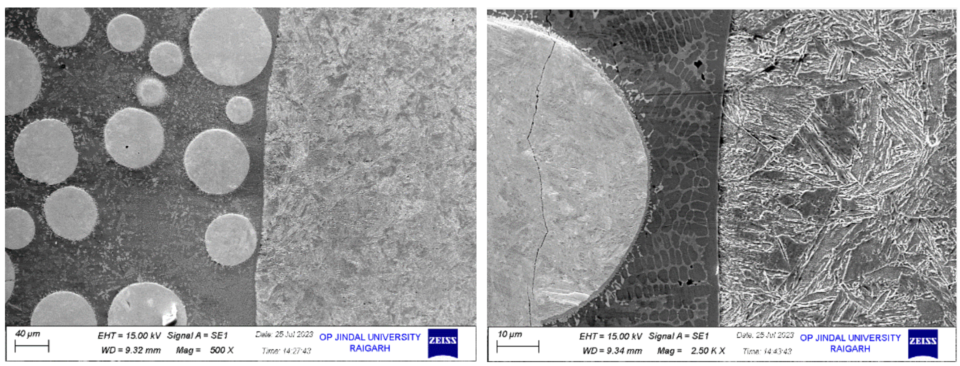

Figure 5. Sample 3: The interface exhibits the metallurgical bonding between steel and Laser Metal Deposition (LMD) of WC-NiCrBSi.

Upon subjecting the Ni matrix to chemical etching using a mixture of 5% HNO3 and 95% Methanol, a distinct dendritic structure emerges. This dendritic structure, in line with the cooling direction, is characterized by a composition of 74% Ni, 6% Cr, and 10% W near the steel substrate. The interface zone, deeper in color, exhibits a composition rich in Fe and Ni. These distinct domains result from complex chemical reactions during the hard facing operation. [47]

The hard facing operation initiates with the liquefaction of the Ni matrix, facilitating the dissolution of WC particles into the molten matrix. During this process, WC particles undergo a transformation, with a discernible reduction in size near the interfaces. This is well-established, as smaller particles tend to exhibit a heightened propensity for dissolution. The liberated carbon (C) from the dissolution of WC diffuses within the liquid matrix, leading to the formation of intermetallic phases with Cr, such as Cr23C6, and eutectic phases involving W2C in the vicinity of WC particle peripheries. These transformations explain the observed increase in microhardness within the hard-faced layers compared to the matrix. [26,27,29,46]

$$W \rightarrow W2C \rightarrow WC \quad (1)$$

The presence of additional phases within the Ni matrix, including W4Ni [31], can be attributed to the high melting point of W and its relatively generous solubility threshold in Ni, as per the W-Ni binary phase diagram. As the temperature recedes, dendritic phases with a high Ni content but low W content form [32].

The entrainment of W within the matrix, fragmentation of diminutive WC particles, and alteration of WC particle morphology collectively poses challenges to the wear resistance of the WC particle-reinforced composite. The formation of intermetallic phases within the Ni matrix results in a reduction in matrix ductility, which can adversely affect wear resistance [26,32].

To mitigate this effect, careful control over the chemical composition and structural attributes of the WC particles, as well as judicious manipulation of matrix alloy parameters, becomes imperative. The size and configuration of WC particles also need to be considered to ensure their equitable dispersion within the matrix. The selection of an appropriate matrix alloy plays a critical role in shaping the wear and abrasive characteristics of the layer, striking a balance among mechanical properties like hardness, strength, and ductility.

The gradual transformation of Ni's microstructure from a dendritic morphology near the substrate to an equiaxial configuration surrounding larger WC particles can be attributed to shifting nucleation mechanisms [30,32]. WC particles serve as heat sources during the cooling process, fostering the formation of equiaxial-shaped phases near the WC particles. The presence of oxides and pores at this interface is influenced by factors such as the interaction of materials with ambient air at elevated temperatures during the thermal spray process and the impact velocity of interface particles.

The interface between the WC-NiCrBSi-Fe alloy hard facing and the steel substrate is seamless, resulting from the interplay of Ni, Cr, Fe, and W [37,39]. SEM line scan analyses reveal shown in the Figure 6–8. the variation in chemical composition along the interfaces. The mutual solubility of these elements, particularly Ni and Fe, contributes to the inter-diffusion across the interface, strengthening the bonding and mitigating stress at the junction.

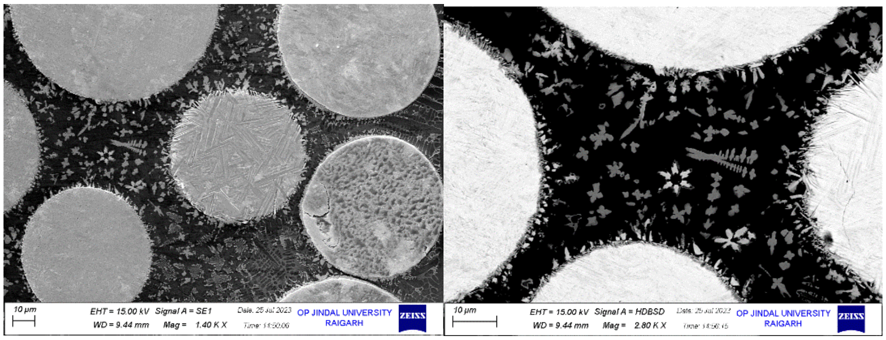

Figure 6. Micro-structure of Laser metal deposition of metal matrix.

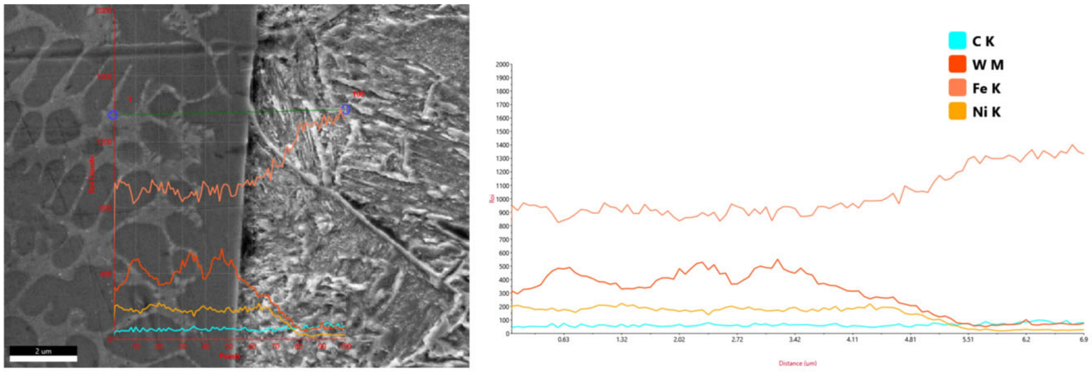

Figure 7. Sample 1 line scan from layer to steel surface; indicates martensite and elemental diffusion.

Preprints (www.preprints.org) | NOT PEER-REVIEWED | Posted: 7 November 2023 doi:10.20944/preprints202311.0486.v1

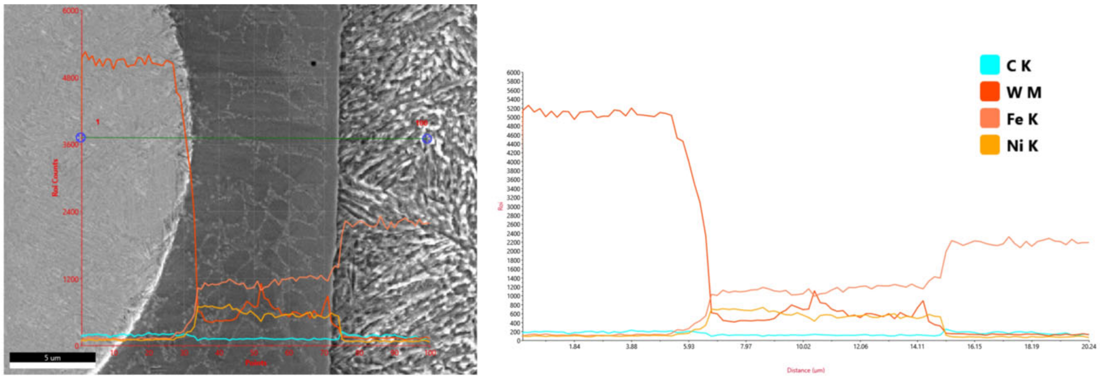

Figure 8. sample 2 Line scan from hardface layer to steel; indicates high carbon martensite in interface drastic tungsten drop at interface.

The SEM EDS analysis provides insight into the microstructural composition of the NiCrBSi coatings and reveals the presence of various phases, including Ni/Ni3B, Cr7C3 carbides, and CrB borides. The microstructure of the composite coatings is complex, with NiCrW solid solutions, WC, Cr7C3, and Cr23C6, along with eutectic phases and oxides. The composition varies depending on the proportion of WC and matrix alloy in the coatings, impacting hardness and other mechanical properties [46].

The microstructure and composition play a crucial role in the wear resistance and performance of hard-facing materials. The transformation of WC particles, the formation of intermetallic phases, and the evolution of microstructure provide insights for optimizing material properties in demanding applications.

The microstructure analysis provides valuable insights into the formation of intermetallic phases, the impact on wear resistance, and the intricate interplay of elements within the material. It also underscores the importance of carefully controlling the composition and structure of WC particles and the choice of the matrix alloy.

The seamless interface between the hard facing layer and the steel substrate is vital in mitigating stress at the junction, contributing to the overall effectiveness of the coating.

Figure 9 presents a comprehensive overview of microhardness depth profiles of coatings fabricated under various processing parameters. Notably, an undulatory pattern is discernible in the hardness values as they traverse different depths in all specimens. This pattern is intricately linked to the stratified microstructure within the molten pool's cross-section. The stratification is influenced by the morphology of structural constituents and the distribution of tungsten-rich carbide precipitates, which impact the concentration of the carbide phase in distinct cross-sectional regions.

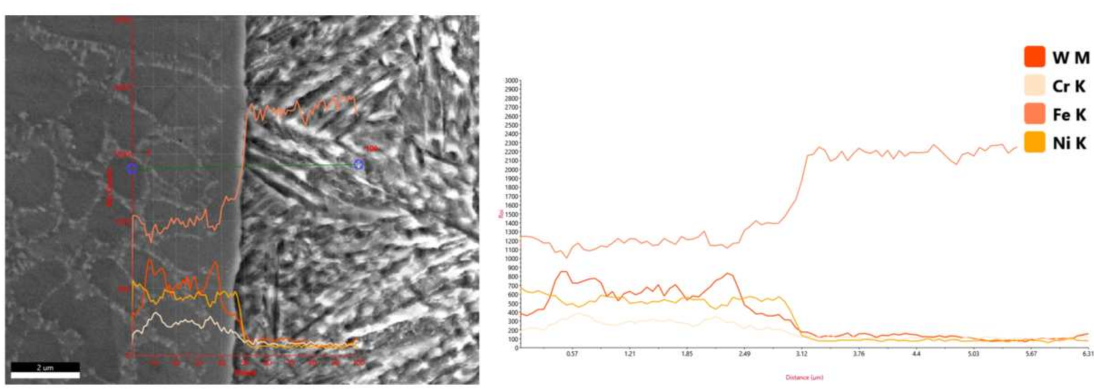

Figure 9. sample 2 Line scan from hard-face layer to steel; indicates high carbon martensite in interface drastic tungsten drop at interface.

The influence of processing parameters on hardness is a critical aspect of our study, as demonstrated in Figure 9. This figure highlights the impact of varying the laser current while maintaining a constant rate, as well as the effect of altering the laser operating speed while keeping the current constant. Notably, our analysis reveals that the average hardness values within the remelted zones exhibit a relatively narrow range, fluctuating between approximately ~1050 HK0.5 and ~1150 HK0.5 across the different samples. This observation underscores the significance of fine-tuning processing parameters to achieve the desired hardness characteristics in laser-clad materials. [5,9,19,35]

Interestingly, there is a reasonable but small decrease in hardness when laser operating speed decreases and laser current increases. This trend correlates harmoniously with the size of the main tungsten-rich phase, as indicated in the Figure 9. Notably, samples 2 and 3, remelted at maximum power density and heat input, exhibit the lowest hardness levels at the interface.

Within samples characterized by a penetration depth exceeding the coating thickness (sample 3), a significant iron concentration of approximately ~16 wt% is observed, nearly threefold higher than its counterparts. This elevated iron concentration results from the extensive intermingling between the coating and substrate materials during the remelting process, coupled with a slightly coarser structure. These factors collectively contribute to the comparatively lower hardness of the remelted layers.

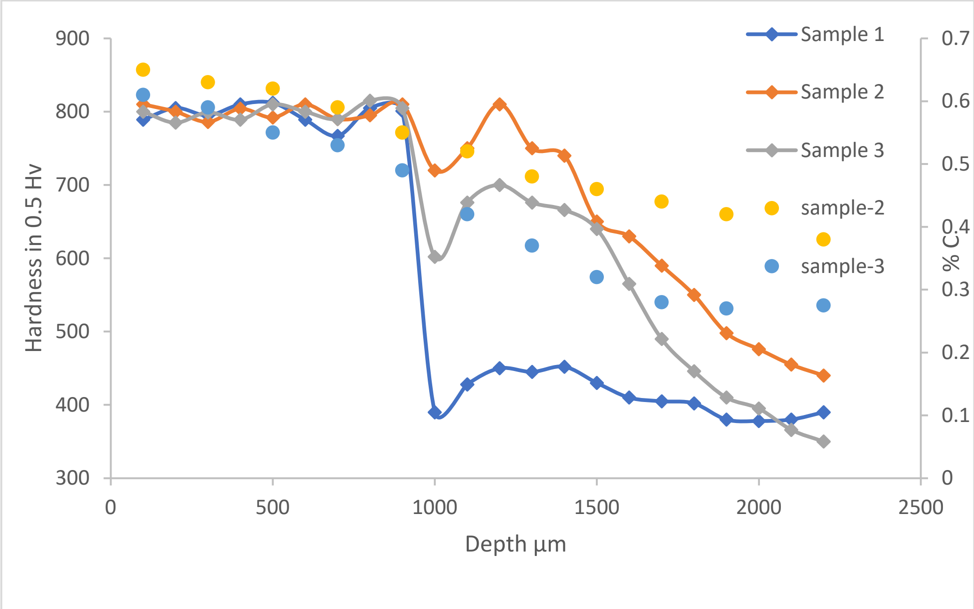

Figure 10. Hardness profile of samples 1, 2, 3, indicating a dip at the interface.

The microhardness depth profiles obtained in our study shed light on the intriguing characteristics of spherical-cast carbides dispersed throughout the coating's microstructure, yielding remarkable hardness levels ranging from 2500 HV to 3100 HV. As depicted in the figures, a distinctive undulatory pattern in hardness values is discernible, closely related to the stratified microstructure within the molten pool [35]. This stratification is intricately woven by the morphology of structural constituents and the distribution of tungsten-rich carbide precipitates, significantly impacting the concentration of the carbide phase in distinct cross-sectional domains. Our findings underscore the intricate relationship between processing parameters and coating hardness, with a reasonable yet discernible decrease in hardness as laser operating speed decreases and laser current increases. Notably, this trend harmonizes with the size of the main tungsten-rich phase. Furthermore, our study elucidates the factors contributing to variations in hardness levels, particularly the extent of intermingling between coating and substrate materials during the remelting process. Understanding these dynamics is pivotal for optimizing the properties of hard-facing materials, where spherical-cast

Preprints (www.preprints.org) | NOT PEER-REVIEWED | Posted: 7 November 2023 doi:10.20944/preprints202311.0486.v1

carbides play a pivotal role in achieving exceptional hardness levels ranging from 2500 HV to 3100 HV distributed throughout the layer.

Conclusions

To sum up, the study uncovered complex patterns from thorough investigation of microhardness depth profiles under different processing settings. Because of the microstructure in the molten pool cross-section, which is impacted by the dispersion of tungsten-rich carbide, the hardness values of the specimen change with its depth. Non-remelted zones also show variations in hardness correlated with splat sizes. It is discovered that in accordance with tungsten-rich phase dimensions, coating hardness is decreased by lower laser speed and greater current. The distribution of tungsten and composition are influenced by coating penetration depth, with mixing being shown in deep penetrations. The study emphasizes that while variations in hardness are significant, the main finding is that all treated coatings perform better than as-sprayed coating and conventional remelting techniques because pulsed lasers produce small microstructures quickly by heating and cooling them. This has expanded possibilities for the mining industry and important ramifications for laser cladding and advanced coatings.

Author Contributions: For research articles with several authors, a short paragraph specifying their individual contributions must be provided. The following statements should be used "Conceptualization, K.V.K. and M.K.P.; methodology, K.V.K.; software, M.K.P.; validation, K.V.K. and M.K.P.; formal analysis, K.V.K. and M.K.P.; investigation, K.V.K. and M.K.P.; resources, K.V.K. and M.K.P.; data curation, K.V.K.; writing—original draft preparation, K.V.K.; writing—review and editing, M.K.P.; visualization, K.V.K.; supervision, M.K.P.; project administration, K.V.K. and M.K.P.; funding acquisition, K.V.K. All authors have read and agreed to the published version of the manuscript.

Funding: no funding was provided.

Acknowledgments: Authors thank Central Instrumentation Facility (CIF) at OP Jindal University for the SEM characterization. VKK thanks Metallurgy staff at OPJU for their support in preparation of the samples.

Conflicts of Interest: I would like to declare there is no conflicts of interest.

References

1. Varun Kumar, K., & Kalyan Phani, M. (2022). Microstructural and mechanical characterization of parallel layered WC- NiCr weld overlay on 080 M40 steel substrate prepared using additive manufacturing. *Materials Today: Proceedings*, *67*, 501–506. https://doi.org/10.1016/j.matpr.2022.06.472
2. da Silva, L. J., & D'Oliveira, A. S. C. (2016, March). NiCrSiBC coatings: Effect of dilution on microstructure and high temperature tribological behavior. *Wear*, *350–351*, 130–140. https://doi.org/10.1016/j.wear.2016.01.015
3. Rachidi, R., El Kihel, B., & Delaunois, F. (2019, February). Microstructure and mechanical characterization of NiCrBSi alloy and NiCrBSi-WC composite coatings produced by flame spraying. *Materials Science and Engineering: B*, *241*, 13–21. https://doi.org/10.1016/j.mseb.2019.02.002
4. Hulka, I., Uțu, I. D., Avram, D., Dan, M. L., Pascu, A., Stanciu, E. M., & Roată, I. C. (2021, September 26). Influence of the Laser Cladding Parameters on the Morphology, Wear and Corrosion Resistance of WC-Co/NiCrBSi Composite Coatings. *Materials*, *14*(19), 5583. https://doi.org/10.3390/ma14195583
5. Škamat, J., Černašėjus, O., Zhetessova, G., Nikonova, T., Zharkevich, O., & Višniakov, N. (2021, October 13). Effect of Laser Processing Parameters on Microstructure, Hardness and Tribology of NiCrCoFeCBSi/WC Coatings. *Materials*, *14*(20), 6034. https://doi.org/10.3390/ma14206034
6. Salimi, A., & Sanjabi, S. (2018, October). Infiltration brazed core-shell WC@NiP/NiCrBSi composite cladding. *Surface and Coatings Technology*, *352*, 59–73. https://doi.org/10.1016/j.surfcoat.2018.08.001
7. Zhou, S., Lei, J., Dai, X., Guo, J., Gu, Z., & Pan, H. (2016, November). A comparative study of the structure and wear resistance of NiCrBSi/50 wt.% WC composite coatings by laser cladding and laser induction hybrid cladding. *International Journal of Refractory Metals and Hard Materials*, *60*, 17–27. https://doi.org/10.1016/j.ijrmhm.2016.06.019
8. Simunovic, K., Slokar, L., & Havrlisan, S. (2016, November 14). SEM/EDS investigation of one-step flame sprayed and fused Ni-based self-fluxing alloy coatings on steel substrates. *Philosophical Magazine*, *97*(4), 248–268. https://doi.org/10.1080/14786435.2016.1257167

9. Deschuyteneer, D., Petit, F., Gonon, M., & Cambier, F. (2015, December). Processing and characterization of laser clad NiCrBSi/WC composite coatings — Influence of microstructure on hardness and wear. *Surface and Coatings Technology*, *283*, 162–171. https://doi.org/10.1016/j.surfcoat.2015.10.055
10. Nowotny, S., Brueckner, F., Thieme, S., Leyens, C., & Beyer, E. (2014, December 9). High-performance laser cladding with combined energy sources. *Journal of Laser Applications*, *27*(S1). https://doi.org/10.2351/1.4817455
11. Brueckner, F., Riede, M., Marquardt, F., Willner, R., Seidel, A., Thieme, S., Leyens, C., & Beyer, E. (2017, May 1). Process characteristics in high-precision laser metal deposition using wire and powder. *Journal of Laser Applications*, *29*(2). https://doi.org/10.2351/1.4983237
12. Shishkovsky, I., Kakovkina, N., & Sherbakof, V. (2020). Mechanical properties of NiCrBSi self-fluxing alloy after LPBF with additional heating. *Procedia CIRP*, *94*, 217–221. https://doi.org/10.1016/j.procir.2020.09.041
13. Simunovic, K., Saric, T., & Simunovic, G. (2014, June 3). Different Approaches to the Investigation and Testing of the Ni-Based Self-Fluxing Alloy Coatings—A Review. Part 1: General Facts, Wear and Corrosion Investigations. *Tribology Transactions*, *57*(6), 955–979. https://doi.org/10.1080/10402004.2014.927547
14. Simunovic, K., Saric, T., & Simunovic, G. (2014, June 3). Different Approaches to the Investigation and Testing of the Ni-Based Self-Fluxing Alloy Coatings—A Review. Part 2: Microstructure, Adhesive Strength, Cracking Behavior, and Residual Stresses Investigations. *Tribology Transactions*, *57*(6), 980–1000. https://doi.org/10.1080/10402004.2014.927548
15. Sbrizher, A. G. (1988, April). Structure and properties of coatings made of self-fluxing alloys. *Metal Science and Heat Treatment*, *30*(4), 296–299. https://doi.org/10.1007/bf00774582
16. Bergant, Z., Trdan, U., & Grum, J. (2014, November). Effect of high-temperature furnace treatment on the microstructure and corrosion behavior of NiCrBSi flame-sprayed coatings. *Corrosion Science*, *88*, 372–386. https://doi.org/10.1016/j.corsci.2014.07.057
17. Chen, J., Dong, Y., Wan, L., Yang, Y., Chu, Z., Zhang, J., He, J., & Li, D. (2018, April). Effect of induction remelting on the microstructure and properties of in situ TiN-reinforced NiCrBSi composite coatings. *Surface and Coatings Technology*, *340*, 159–166. https://doi.org/10.1016/j.surfcoat.2018.02.024
18. Deschuyteneer, D., Petit, F., Gonon, M., & Cambier, F. (2017, February). Influence of large particle size – up to 1.2 mm – and morphology on wear resistance in NiCrBSi/WC laser cladded composite coatings. *Surface and Coatings Technology*, *311*, 365–373. https://doi.org/10.1016/j.surfcoat.2016.12.110
19. Deschuyteneer, D., Petit, F., Gonon, M., & Cambier, F. (2015, December). Processing and characterization of laser clad NiCrBSi/WC composite coatings — Influence of microstructure on hardness and wear. *Surface and Coatings Technology*, *283*, 162–171. https://doi.org/10.1016/j.surfcoat.2015.10.055
20. Buytoz, S., Ulutan, M., Islak, S., Kurt, B., & Nuri Çelik, O. (2013, February 1). Microstructural and Wear Characteristics of High Velocity Oxygen Fuel (HVOF) Sprayed NiCrBSi–SiC Composite Coating on SAE 1030 Steel. *Arabian Journal for Science and Engineering*, *38*(6), 1481–1491. https://doi.org/10.1007/s13369-013-0536-y
21. Sun, R., Lei, Y., & Niu, W. (2009, February). Laser clad TiC reinforced NiCrBSi composite coatings on Ti–6Al–4V alloy using a CW CO2 laser. *Surface and Coatings Technology*, *203*(10–11), 1395–1399. https://doi.org/10.1016/j.surfcoat.2008.11.012
22. Shabana, Sarcar, M., Suman, K., & Kamaluddin, S. (2015). Tribological and Corrosion behavior of HVOF Sprayed WC-Co, NiCrBSi and Cr3C2-NiCr Coatings and analysis using Design of Experiments. *Materials Today: Proceedings*, *2*(4–5), 2654–2665. https://doi.org/10.1016/j.matpr.2015.07.227
23. CAI, B., TAN, Y. F., TAN, H., JING, Q. F., & ZHANG, Z. W. (2013, July). Tribological behavior and mechanism of NiCrBSi–Y2O3 composite coatings. *Transactions of Nonferrous Metals Society of China*, *23*(7), 2002–2010. https://doi.org/10.1016/s1003-6326(13)62689-8
24. Hemmati, I., Rao, J., Ocelík, V., & De Hosson, J. (2013, January 25). Electron Microscopy Characterization of Ni-Cr-B-Si-C Laser Deposited Coatings. *Microscopy and Microanalysis*, *19*(1), 120–131. https://doi.org/10.1017/s1431927612013839
25. Chen, L. Y., Xu, T., Wang, H., Sang, P., Lu, S., Wang, Z. X., Chen, S., & Zhang, L. C. (2019, January). Phase interaction induced texture in a plasma sprayed-remelted NiCrBSi coating during solidification: An electron backscatter diffraction study. *Surface and Coatings Technology*, *358*, 467–480. https://doi.org/10.1016/j.surfcoat.2018.11.019
26. Sheppard, P., & Koiprasert, H. (2014, September). Effect of W dissolution in NiCrBSi–WC and NiBSi–WC arc sprayed coatings on wear behaviors. *Wear*, *317*(1–2), 194–200. https://doi.org/10.1016/j.wear.2014.06.008
27. Zhou, S., & Dai, X. (2010, May). Laser induction hybrid rapid cladding of WC particles reinforced NiCrBSi composite coatings. *Applied Surface Science*, *256*(14), 4708–4714. https://doi.org/10.1016/j.apsusc.2010.02.078
28. Bergant, Z., & Grum, J. (2009, February 27). Quality Improvement of Flame Sprayed, Heat Treated, and Remelted NiCrBSi Coatings. *Journal of Thermal Spray Technology*, *18*(3), 380–391. https://doi.org/10.1007/s11666-009-9304-7

29. Fernández, M., García, A., Cuetos, J., González, R., Noriega, A., & Cadenas, M. (2015, February). Effect of actual WC content on the reciprocating wear of a laser cladding NiCrBSi alloy reinforced with WC. *Wear*, *324–325*, 80–89. https://doi.org/10.1016/j.wear.2014.12.021
30. Ahmed, M. M. Z., Barakat, W. S., Y. A. Mohamed, A., A. Alsaleh, N., & Elkady, O. A. (2021, February 6). The Development of WC-Based Composite Tools for Friction Stir Welding of High-Softening-Temperature Materials. *Metals*, *11*(2), 285. https://doi.org/10.3390/met11020285
31. Lin, N., Jiang, Y., Zhang, D., Wu, C., He, Y., & Xiao, D. (2011, July). Effect of Cu, Ni on the property and microstructure of ultrafine WC-10Co alloys by sinter–hipping. *International Journal of Refractory Metals and Hard Materials*, *29*(4), 509–515. https://doi.org/10.1016/j.ijrmhm.2011.02.012
32. Yao, S. H. (2014, May). Tribological behaviour of NiCrBSi–WC(Co) coatings. *Materials Research Innovations*, *18*(sup2), S2-332. https://doi.org/10.1179/1432891714z.000000000436
33. Vencl, A., Mrdak, M., & Hvizdos, P. (2017, June). Tribological Properties of WC-Co/NiCrBSi and Mo/NiCrBSi Plasma Spray Coatings under Boundary Lubrication Conditions. *Tribology in Industry*, *39*(2), 183–191. https://doi.org/10.24874/ti.2017.39.02.04
34. Bolelli, G., Börner, T., Milanti, A., Lusvarghi, L., Laurila, J., Koivuluoto, H., Niemi, K., & Vuoristo, P. (2014, June). Tribological behavior of HVOF- and HVAF-sprayed composite coatings based on Fe-Alloy+WC–12% Co. *Surface and Coatings Technology*, *248*, 104–112. https://doi.org/10.1016/j.surfcoat.2014.03.037
35. Armstrong, R. W. (2011, July 14). The Hardness and Strength Properties of WC-Co Composites. *Materials*, *4*(7), 1287–1308. https://doi.org/10.3390/ma4071287
36. Valsecchi, B., Previtali, B., Vedani, M., & Vimercati, G. (2010, April). Fiber Laser Cladding with High Content of WC-Co Based Powder. *International Journal of Material Forming*, *3*(S1), 1127–1130. https://doi.org/10.1007/s12289-010-0970-2
37. Cadenas, M., Vijande, R., Montes, H., & Sierra, J. (1997, December). Wear behaviour of laser cladded and plasma sprayed WC⊚Co coatings. *Wear*, *212*(2), 244–253. https://doi.org/10.1016/s0043-1648(97)00127-0
38. Mühlbauer, G., Kremser, G., Bock, A., Weidow, J., & Schubert, W. D. (2018, April). Transition of W 2 C to WC during carburization of tungsten metal powder. *International Journal of Refractory Metals and Hard Materials*, *72*, 141–148. https://doi.org/10.1016/j.ijrmhm.2017.12.018
39. Niranatlumpong, P., & Koiprasert, H. (2011, October). Phase transformation of NiCrBSi–WC and NiBSi–WC arc sprayed coatings. *Surface and Coatings Technology*, *206*(2–3), 440–445. https://doi.org/10.1016/j.surfcoat.2011.07.057
40. Bergant, Z., & Grum, J. (2011, March 1). POROSITY EVALUATION OF FLAME-SPRAYED AND HEAT-TREATED NICKEL-BASED COATINGS USING IMAGE ANALYSIS. *Image Analysis & Stereology*, *30*(1), 53. https://doi.org/10.5566/ias.v30.p53-62
41. Paul, C., Alemohammad, H., Toyserkani, E., Khajepour, A., & Corbin, S. (2007, August). Cladding of WC–12 Co on low carbon steel using a pulsed Nd:YAG laser. *Materials Science and Engineering: A*, *464*(1–2), 170–176. https://doi.org/10.1016/j.msea.2007.01.132
42. Wu, X., Zhu, B., Zeng, X., Hu, X., & Cui, K. (1996, February). Critical state of laser cladding with powder auto-feeding. *Surface and Coatings Technology*, *79*(1–3), 200–204. https://doi.org/10.1016/0257-8972(95)02452-2
43. Khafidh, M., Schipper, D., Masen, M., Vleugels, N., & Noordermeer, J. (2018, June 30). Tribological behavior of short-cut aramid fiber reinforced SBR elastomers: the effect of fiber orientation. *JOURNAL OF MECHANICAL ENGINEERING AND SCIENCES*, *12*(2), 3700–3711. https://doi.org/10.15282/jmes.12.2.2018.15.0327
44. Indhu, R., Vivek, V., Sarathkumar, L., Bharatish, A., & Soundarapandian, S. (2018, October 22). Overview of Laser Absorptivity Measurement Techniques for Material Processing. *Lasers in Manufacturing and Materials Processing*, *5*(4), 458–481. https://doi.org/10.1007/s40516-018-0075-1
45. Schneider, M., Berthe, L., Fabbro, R., & Muller, M. (2008, June 26). Measurement of laser absorptivity for operating parameters characteristic of laser drilling regime. *Journal of Physics D: Applied Physics*, *41*(15), 155502. https://doi.org/10.1088/0022-3727/41/15/155502

 doi:10.20944/preprints202311.0486.v1

46. Bergant, Z., Batič, B. E., Felde, I., Šturm, R., & Sedlaček, M. (2022, January 4). Tribological Properties of Solid Solution Strengthened Laser Cladded NiCrBSi/WC-12Co Metal Matrix Composite Coatings. *Materials*, *15*(1), 342. https://doi.org/10.3390/ma15010342
47. Karimzadeh, A., Aliofkhazraei, M., & Walsh, F. C. (2019, August). A review of electrodeposited Ni-Co alloy and composite coatings: Microstructure, properties and applications. *Surface and Coatings Technology*, *372*, 463–498. https://doi.org/10.1016/j.surfcoat.2019.04.079